

Chapter 11

Design Optimization of the Primary Pump of a Nuclear Reactor

T. Verstraete and L. Mueller

Abstract Engineers are often challenged by designing new equipment without any prior knowledge or guidance from an existing similar product. The large degree of freedom that this generates can become a bottleneck as it could lead to a loss of global oversight and may even lead to wrong, uninformed choices. It is essential to have a large exploration of the design space to allow for innovative solutions, on the other hand it is important to introduce a high level of detail as early as possible in the design process to increase the reliability of the model predictions, which drive the decision process. This leads to a well-known conflict where more knowledge is needed upfront in the design process in the early stages of the design, and a larger degree of freedom is needed near the end of the design process where typically more knowledge is available. In this work it is demonstrated how modern design optimization tools can be effectively used to integrate the preliminary with the detailed design process. The key to achieve a good balance between design exploration and detailed design is obtained by reducing the parameters that are fixed during the preliminary design to an absolute minimum, such that the detailed design phase has still a large degree of freedom. The parameters that are fixed in the preliminary design phase are moreover those parameters that have a pronounced influence on the design performance and can be reliably predicted by a lower detail analysis code. Both preliminary and detailed design processes rely heavily on optimization techniques. Due to the larger computational cost in the detailed design phase, a surrogate model based optimization is used opposed to an evolutionary algorithm in the preliminary design phase. The application within this paper is the design of a liquid-metal pump for the primary cooling system of the advanced nuclear reactor MYRRHA conceived by the Belgian research center (SCK-CEN). This single stage axial-flow pump has unique design requirements not met by any previously designed pump, and hence demands for a novel approach.

T. Verstraete (✉) · L. Mueller

Turbomachinery and Propulsion Department, von Karman Institute for Fluid Dynamics,
Waterloosesteenweg 72, B-1640 Sint-Genesius-Rode, Belgium
e-mail: tom.verstraete@vki.ac.be

L. Mueller

e-mail: lasse.mueller@vki.ac.be

© Springer International Publishing Switzerland 2015

D. Greiner et al. (eds.), *Advances in Evolutionary and Deterministic Methods for Design, Optimization and Control in Engineering and Sciences*, Computational Methods in Applied Sciences 36, DOI 10.1007/978-3-319-11541-2_11

Keywords Turbomachinery · Design optimization · Computational fluid dynamics

11.1 Introduction

The MYRRHA project, initiated by the Belgian nuclear research center (SCK·CEN), aims at demonstrating a new generation of nuclear reactors. Indeed, fourth generation fast reactors show considerable improvements in fuel efficiency, safety and nuclear waste generation compared to the current installed reactors. The primary coolant is either sodium or lead/lead-bismuth eutectic (LBE). The use of sodium has more safety hazards as it reacts explosively with water and ignites in air, and has a lower boiling point. In contrast, the main problem with LBE is related to erosion.

The MYRRHA reactor is conceived as an accelerator driven system (ADS), able to operate in sub-critical and critical modes [7] and will allow the demonstration and performance assessment of the transmutation concept and associated technologies starting in 2023.

The primary system of the MYRRHA research reactor is a pool-type design, as illustrated in Fig. 11.1. All components of the primary loop, i.e. the pumps, heat exchangers, fuel handling tools, experimental rigs, etc., are inserted from the top and immersed in the reactor vessel, which is filled with lead-bismuth eutectic (LBE) as primary coolant. The relatively high boiling temperature of LBE of 1,670 °C leads

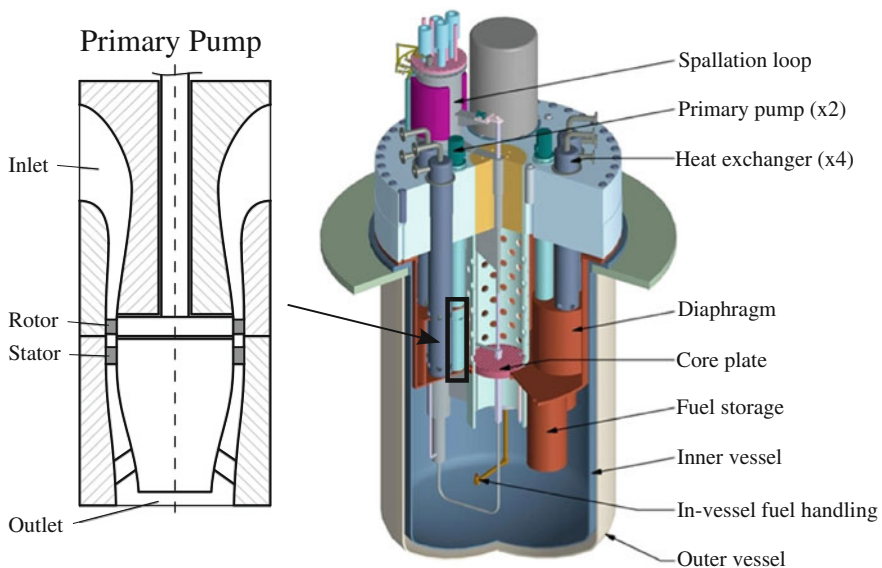


Fig. 11.1 Schematic assembly of the MYRRHA reactor [7] with a close up of the primary pump (dimensions not to scale)

to a passively safe design regarding a loss of coolant accident (LOCA), as it allows the operation without pressurizing the reactor even at high temperatures. However, the high density of $10,000 \text{ kg/m}^3$ and the corrosive properties of LBE add additional challenges to the design, which regard mainly a restriction in flow velocity. Lower flow velocities will for instance reduce the convective heat transfer, hence resulting in large heat exchangers. But more significantly, low flow velocities have a major impact on the pump design reducing dramatically the realizable head. The maximum relative velocity in the pump needs indeed to be limited to rather low values to avoid excessive blade erosion, e.g. it is reported that pumps developed by OKBM [6] for nuclear submarines operate at maximum velocities of $W_{max} = 25\text{--}30 \text{ m/s}$.

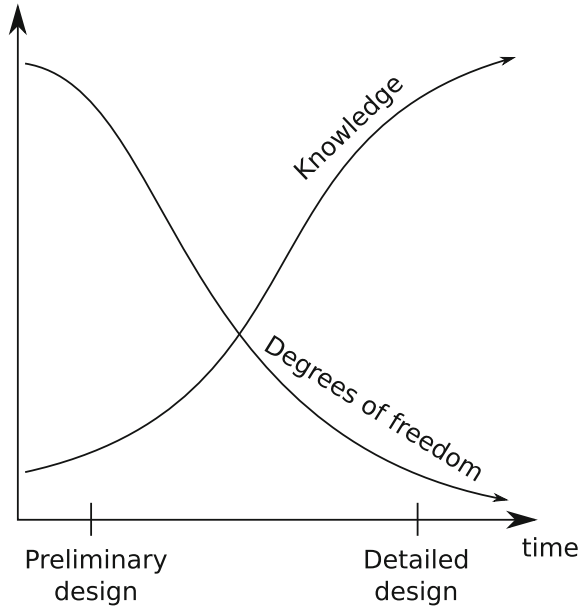
11.2 Design Procedure

Reducing the maximum velocity to limit erosion is an essential and unique objective to be addressed in the design of the primary pump. Up to this date, such pumps have only been designed for Soviet Alfa class nuclear submarines during the 1970s and no detailed reports on the design of such pumps exists. Hence one cannot rely on any previous experience for the design, necessitating a thorough study of how the particular requirements can be met.

As a design process evolves over time, more and more design parameters are fixed limiting the remaining degrees of freedom. However, knowledge on the design is gathered over the course of the design process and builds up mainly after the preliminary design stage, as shown graphically in Fig. 11.2. This means that important decisions have to be taken at early stages in the design process where only limited information is available, which may lead to poorly informed decisions. It is therefore advisable to limit as much as possible the decisions made early in the design process while gathering as much knowledge as possible.

In this work it was therefore intended to limit the degree of freedom as much as possible in the early design phase. To this end, the design process was split in two sequential phases, each relying on modern optimization techniques. The first stage consisted of a preliminary design phase where the type of pump and global dimensions were fixed. The following phase consisted in a detailed design optimization of the pump shape, keeping only few parameters fixed as defined from the preliminary design phase. Such approach allows to prevent premature conclusions to be drawn in the early design phase where only limited models are used, but on the other hand still allows for a reasonably manageable optimization problem in the detailed design phase where the main interactions between the different design parameters is limited. Indeed, it is well known that the complexity of optimization problems increases the higher the degree of interaction is between the different design variables. Within this work, the most interfering design parameters have been fixed during the preliminary analysis, which is possible since they can be well represented by lower accuracy analysis tools.

Fig. 11.2 Degrees of freedom and acquisition of knowledge during design



A fully detailed design optimization from the start, without any preliminary design phase, is practically impossible. The large degree of freedom, combined with high order interactions between several parameters, lead to a very complicated design space that requires a high level of evaluations to accurately cover the myriad of design options.

11.3 Preliminary Design Optimization

11.3.1 Machine Type

The preliminary design phase starts by the selection of the machine type. For pumps a wide choice of different machine types exists. In the present work volumetric (or positive displacement) pumps are ruled out for maintenance and other reasons. The most attractive pump type is a rotodynamic pump which still has a large choice of machine type (axial flow, mixed flow, or radial flow). This choice is mainly related to the design requirements of the pump, i.e. to the flow rate Q and the total head ΔH . A classical parameter in the selection of hydraulic machinery is the specific speed

$$N_s = \frac{RPM \sqrt{Q}}{\Delta H^{3/4}}. \quad (11.1)$$

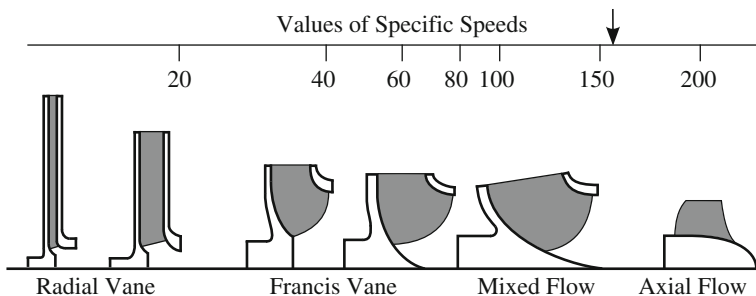


Fig. 11.3 Specific speed chart

This specific speed is used as a guideline for the selection of the machine type based on a large database of existing designs. It suggests a type of machine that should deliver the highest efficiency for the required specific speed. This should be viewed as a strong suggestion, however one may deviate from the suggested type with the risk of having a lower efficiency.

Based on the design requirements of the MYRRHA pump provided by SCK-CEN the specific speed is in the range of mixed to axial-flow pumps $N_s \approx 156$ (see Fig. 11.3). Although towards lower RPM a mixed-flow configuration might provide higher efficiency, an axial-flow pump is regarded as the best trade-off solution due its lower mechanical complexity and simplified manufacturing.

The use of charts as Fig. 11.3 is very helpful in the preliminary design phase, as it gives a clear indication for the choice of machinery in terms of global performance parameters. Such charts do however not guarantee the identification of a global optimum and provide no detailed shape. Moreover, no chart exists for the erosion induced requirement of low relative velocity with respect to the walls.

With respect to this requirement, it was decided to analyze various design options in this preliminary design phase. For that reason a simple one-dimensional model has been applied in the hub, mid, and tip section of the rotor to assess the meridional flow path and its rotational speed (Fig. 11.4, left). This rather simple model based on velocity triangles up- and downstream of the rotor blade allows a rapid screening of several design parameters, such as blade angles, rotational speed (RPM), and hub and tip radii, R_{hub} and R_{tip} , respectively. Although it does not include complex flow features, e.g. flow deviation or even flow separation, it provides a good estimation of the initial rotor design as an input for the following detailed 3D-optimization.

Input parameters to the 3D-optimization are the hub and tip radii (R_{hub} and R_{tip}) and the RPM of the rotor as illustrated in Fig. 11.4 (right). These parameters were unchanged in the subsequent detailed high fidelity 3D-optimization, in which the three dimensional design of the pump comprising the inlet section, the rotor and stator rows, and the diffuser has been performed. It is important to note that these three design variables have a large effect on all other design parameters for the detailed design process. Flow angles will change for instance with different rotational speeds, as well as with higher or lower hub and tip radii. To account for such changes, a much

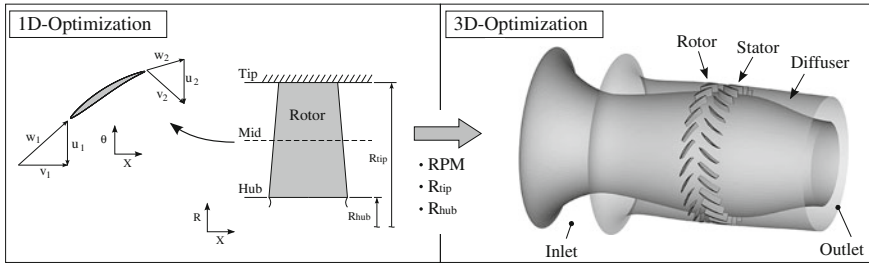


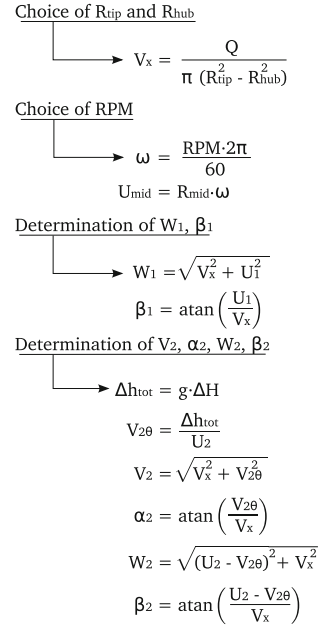
Fig. 11.4 Design procedure

wider range for the blade metal angles will be needed, which is increasing the design space. Additionally, the optimal value for blade angle will depend largely on these three parameters, and hence will require a much larger number of design evaluations with the used methodology to find the optimal value. This can be easily understood as follows: Suppose a sampling technique is used to find the optimum, i.e. the design space is probed in discrete points. When two design variables have no interaction, it is sufficient to put experiments on the diagonal of the design space spanning these two design variables to find the optimum. However, if a strong interaction exists, only sampling the diagonal is not sufficient as it would not allow to see the effect of changing one design variable while keeping the other constant (and necessary if the optimum is in an opposite corner of the diagonal). As such, the entire 2D space spanned by both design variables will need to be sampled. It can be reasonably assumed that most parameters in a 3D design of the axial pump, as will be shown later, have only a low level of interaction with other parameters, and hence result in a relatively easy optimization process. This situation would dramatically change if hub and tip radii and RPM would be added as design variables.

11.3.2 Computational Model

The 1D computational model is illustrated in Fig. 11.5. Input parameters are the hub and tip radii, R_{hub} and R_{tip} , and the RPM, next to the pump requirements (ΔH and Q). The axial velocity V_x is derived from the hub and tip radius for the specified flow rate Q . It is assumed at this stage that the axial velocity upstream of the rotor is constant from hub to tip although the pump will have a radial inlet bend (see Fig. 11.1).

The peripheral speed U is computed at three sections (hub, mid and tip) from the rotational speed and the respective radii. The mid section is positioned in the middle of the hub and tip radius: $R_{mid} = 0.5 \cdot (R_{hub} + R_{tip})$.

Fig. 11.5 1D computational model

The inlet absolute velocity V_1 is assumed to be axial (no pre-rotation), which allows to compute the relative velocity W_1 and the relative flow angle β_1 .

The quantities downstream of the rotor (index 2) are computed based on the required total head ΔH and assuming no losses ($\eta_{hyd} = 1.0$) using the Euler-equation for pure axial inlet flow ($V_{1\theta} = 0$)

$$\frac{g \cdot \Delta H}{\eta_{hyd}} = U_2 V_{2\theta} - U_1 V_{1\theta} = U_2 V_{2\theta} . \quad (11.2)$$

and assuming the axial velocity V_x to maintain constant through the rotor (i.e. free vortex design). The absolute velocity downstream of the rotor V_2 , the absolute flow angle α_2 , the relative velocity W_2 , and the relative flow angle β_2 are computed as illustrated in Fig. 11.5.

11.3.3 Objectives and Constraints

Three design parameters (hub radius R_{hub} , tip radius R_{tip} , and RPM) can be chosen to obtain the required total head ΔH and flow rate Q . However, additional requirements need to be imposed:

- The turning of the flow in the rotor ($\beta_2 - \beta_1$) needs to be limited to reduce the losses, not accounted for in this preliminary design phase. According to [9] the turning is limited to 30–25°.
- The diffusion in the rotor (W_2/W_1) needs to remain feasible. A limit of 0.72 is often used, known as the de Haller number [8].
- The maximum relative velocity in the rotor W_{max} needs to remain at low values (10–20 m/s) to limit erosion.
- The absolute exit flow angle (α_2) needs to be small (from axial direction) to perform a feasible diffusion in the subsequent stator [9].

The corresponding optimization problem is formulated as:

$$\text{Minimize: } Obj_1 = W_1^{tip} \quad (11.3)$$

$$Obj_2 = -W_2^{hub} / W_1^{hub} \quad (11.4)$$

$$\text{Subject to: } Constr_1 = abs(\beta_2^{hub} - \beta_1^{hub}) \leq \Delta\beta_{max} \quad (11.5)$$

$$Constr_2 = V_x \leq V_{x,max} \quad (11.6)$$

The first objective Obj_1 (Eq. 11.3) reduces the maximum relative velocity in the rotor, which is in the tip section at the inlet. A value in the range of $W_1^{tip} = 10\text{--}20$ m/s is considered as feasible, although lower values are preferred, as they would increase the lifetime with respect to erosion. The second objective Obj_2 (Eq. 11.4) maximizes the diffusion ratio near the hub to prevent an excessive diffusion. For a free vortex design the highest diffusion occurs in the hub section. The first constraint (Eq. 11.5) restricts the turning at the hub, where the largest relative flow turning will take place, while the second constraint (Eq. 11.6) puts an additional limitation on the axial velocity to limit the erosion risk in the meridional passage.

11.3.4 Methodology

Three different design variables are allowed to be changed during the preliminary design phase, i.e. the hub and tip radii (R_{hub} and R_{tip}) and the rotational speed RPM. Each design variable is allowed to change within a specified range. For each choice of the hub radius R_{hub} , tip radius R_{tip} , and RPM, the velocity triangles can be computed by the 1D model and the requirements can be evaluated. In order to find the three design parameters that give a suitable compromise for the diffusion W_2/W_1 , turning $\Delta\beta$, and maximum velocity W_{max} requirements, a Differential Evolutionary (DE) algorithm [10] has been used. Figure 11.6 illustrates schematically the optimization flowchart.

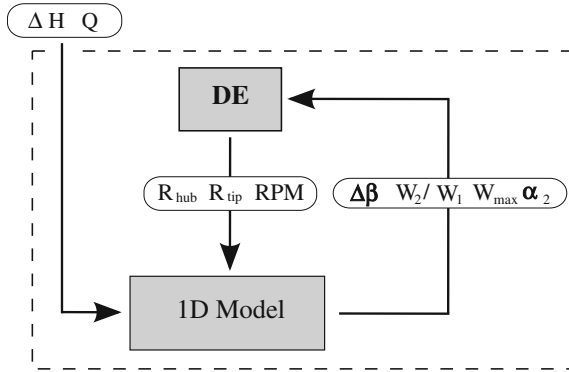


Fig. 11.6 1D optimization flowchart

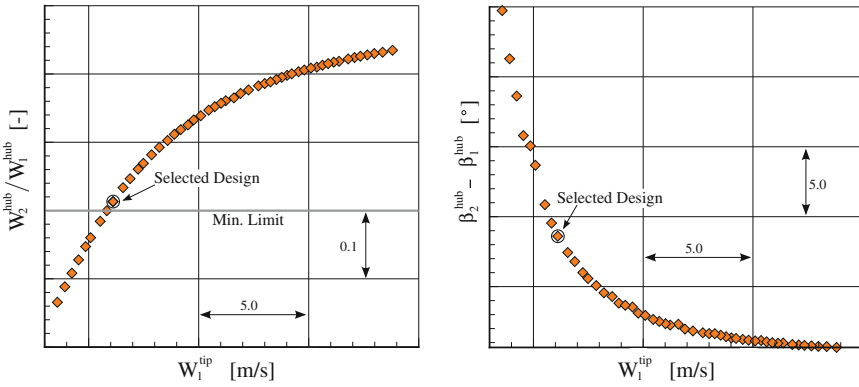


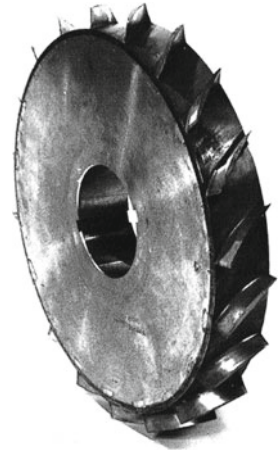
Fig. 11.7 Diffusion in the hub versus relative velocity in the tip section (left), turning in the hub section versus relative velocity in the tip section (right)

11.3.5 Results

The results of the 1D optimization are illustrated in Fig. 11.7, showing both the diffusion in the hub section W_2^{hub}/W_1^{hub} (left) and the flow turning $\beta_2^{hub} - \beta_1^{hub}$ (right) with respect to the relative velocity in the rotor tip section W_1^{tip} . A Pareto front is found with non-dominated designs, in which one objective cannot be improved without worsening the other.

In Fig. 11.7 (left), a clear Pareto front (towards the upper left hand corner) is visible indicating that a lower maximum velocity W_1^{tip} comes at the expense of a larger diffusion near the hub (lower W_2^{hub}/W_1^{hub}). This evidently results also in a higher flow turning near the hub, as can be seen in Fig. 11.7 (right). The resulting Pareto front allows the designer to select designs depending on the weight given to each objective. In the present case, it was decided to select the design with a hub diffusion ratio (W_2^{hub}/W_1^{hub}) close to the minimum limit as indicated in Fig. 11.7 (left).

Fig. 11.8 NASA axial pump rotor for liquid rocket application (hub-to-tip ratio $\nu = 0.9$) [11]



This design has a specific speed of $N_s \approx 70$ with a high hub-to-tip ratio of $\nu = R_{hub}/R_{tip} = 0.88$, which is larger than commonly used for axial (propeller-like) pumps in the range of $\nu = 0.3\text{--}0.7$ [9]. However, this is due to the very low velocity requirement (i.e. low V_x and W_1^{tip}) and high diffusion (i.e. low W_2^{hub}/W_1^{hub}) for a single stage pump. Similar conclusions were drawn within a design study of axial pump rotors for liquid rocket application [1, 3, 11]. Several rotors (see Fig. 11.8) were designed and tested with hub-to-tip ratios between $\nu = 0.4\text{--}0.9$ for a specified diffusion, which confirms the results obtained from this preliminary design optimization.

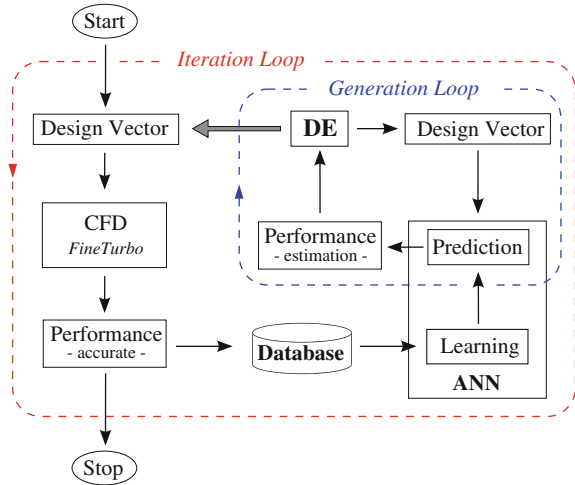
11.4 Detailed Design Optimization

11.4.1 Methodology

The 3D design of the primary pump is performed with the optimization algorithm developed at the von Karman Institute (VKI) with special focus on turbomachinery applications. The system (Fig. 11.9) makes use of a Differential Evolution algorithm (DE), a metamodel based on an Artificial Neural Network (ANN), a database, and high fidelity simulation tools for the flow analysis (CFD).

The basic approach of this method is that the Artificial Neural Network substitutes the computational expensive tools for the CFD in the *Generation Loop* (see Fig. 11.9) and provides less accurate but very fast performance predictions to evaluate the large number of geometries necessary by the DE during its search for the optimum. However, the metamodel requires a validation which is then performed in the *Iteration Loop* according to Fig. 11.9. After a specified number of generations, the optimum

Fig. 11.9 VKI optimization algorithm



geometries according to the ANN predictions are analyzed by the more accurate but much more computationally expensive CFD calculations to verify the accuracy of the metamodel. The results of the accurate performance analysis are added to the database and a new *Generation Loop* is started after a new training of the metamodel on the enlarged database. In this way the whole system is self-learning, resulting in a more accurate ANN.

The Differential Evolution algorithm used was developed by Storn and Price [10]. In present optimization, 1,000 generations are created with a constant population size of 40 individuals. To validate the ANN predictions in each *Iteration Loop* eight individuals were selected and reassessed by the high fidelity tools.

The initial sampling of the database was performed by means of a Design of Experiments (DOE) [4]. The DOE is based on statistical methods and considers, that k design variables can take two values fixed at a specified position in the design space (here: 20 and 80% plus one central case = 50%). Further, to reduce the number of required evaluations, the fractional factorial design approach [4] is used: $2^{(k-p)}$ with $(k - p) = 6$, thus resulting in 64 experiments plus the central case, which are the initial sampling of the database. This clearly illustrates that this method is only working properly if a low level of interactions between the different parameters is present. This justifies the choice of keeping the R_{hub} , R_{tip} and RPM parameters constant after the preliminary analysis.

11.4.2 Parametrization

The 3D model of the rotor of the pump (cf. Fig. 11.1) is based on Bézier and B-spline curves and surfaces and is defined by:

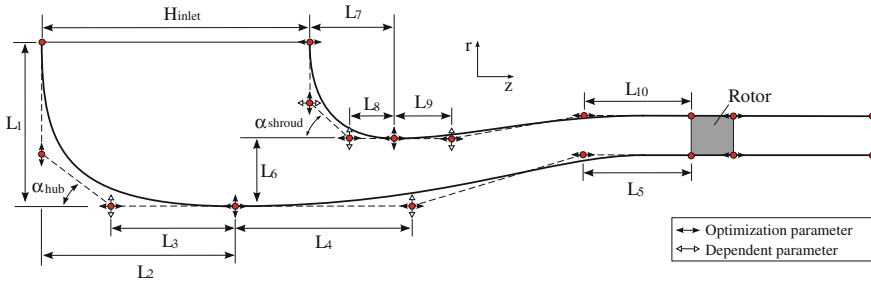


Fig. 11.10 Meridional parametrization of the inlet section and the rotor

1. the meridional contour,
2. the blade camber line at hub and tip,
3. the thickness distribution, which is added normal to the camber line at hub and tip, and
4. the number of blades.

The definition of the meridional contour is shown in Fig. 11.10. The meridional flow path is subdivided into different patches: an inlet patch (90°-bend and swan neck), a blade patch, and an outlet patch. The blade patch corresponds to where the rotor blade is located in the meridional plane. The coordinates of the control points are the geometrical parameters which can be modified by the optimization program and the possible variation in axial and radial direction is indicated by arrows. In order to have a good control about the geometry and to avoid undesirable shapes, lengths and angles are used (e.g. L_1 to L_{10} , H_{inlet} , α_{hub} and α_{shroud}). In total 15 parameters define the meridional flow path.

The rotor blade is defined by the blade camber line of the hub and tip section, each separately defined by the blade angle β_m -distribution with respect to the meridional plane. The β_m -distribution is parametrized by a Bézier curve with three control points, one at the leading and trailing edge and one intermediate control point. This results in a total of 6 degrees of freedom.

The final blade with the pressure and suction side surfaces is created by adding a thickness distribution normal to the camber line at hub and tip. In the present optimization study, a NACA 65 thickness distribution at hub and tip has been chosen, which shape is kept constant during the optimization process.

The number of blades, which defines the full rotor, is introduced as an optimization parameter within this design study. This parameter has a major effect on solidity, i.e. on the blade loading and on the blockage of the flow in case of accidents with no pump rotation, in which cooling needs to be guaranteed by natural convection in the reactor.

In total 22 parameters define the geometry of the pump and will be subject to optimization.

11.4.3 Flow Analysis

Every geometry in the *Iteration Loop* according to Fig. 11.9 has been analyzed at the design operating point using the commercial flow solver fineTurbo™. The incompressible Reynolds-Averaged Navier-Stokes (RANS) equations are solved using a Runge-Kutta scheme in conjunction with accelerating techniques such as variable-coefficient implicit residual smoothing and a multi-grid scheme. Discretization is based on finite volumes with a cell-centered scheme stabilized by artificial dissipation. For the turbulence closure the one equation model of Spalart and Allmaras [12] is used with the assumption of fully turbulent flow with an inlet Reynolds number of

$$Re_{inlet} = \frac{V_{inlet} R_{inlet} \rho}{\mu} = 6.5 \cdot 10^5 \quad (11.7)$$

where V_{inlet} and R_{inlet} are the absolute inlet velocity and the inlet radius, respectively. The flow properties of lead-bismuth eutectic (LBE) according to [5] have been used for the CFD simulations.

11.4.4 Objectives and Constraints

The optimization of the inlet section and the rotor has two objectives:

1. Maximizing the hydraulic efficiency

$$Obj_1 = \eta_{hyd} = \frac{\Delta P_{tot}}{\rho \cdot \Delta(V_\theta U)} \quad (11.8)$$

where ρ is the density of LBE, ΔP_{tot} the mass-flow averaged absolute total pressure rise, and $\Delta(V_\theta U)$ the difference of the mass flow averaged angular momentum between inlet and outlet.

2. Reducing the maximum isentropic velocity $(W/W_0)_{max,SS}$ on the blade suction side at 90% span. The isentropic velocity objective aims at reducing the maximum relative velocity in the tip section (90%-span) as shown in Fig. 11.11 and is computed as follows:

$$Obj_2 = (W/W_0)_{max,SS} = \sqrt{1 - C_p|_{min,SS}} \quad (11.9)$$

with the pressure coefficient C_p :

$$C_p = \frac{P - P_{ref}}{0.5 \cdot \rho \cdot W_{ref}^2} \quad (11.10)$$

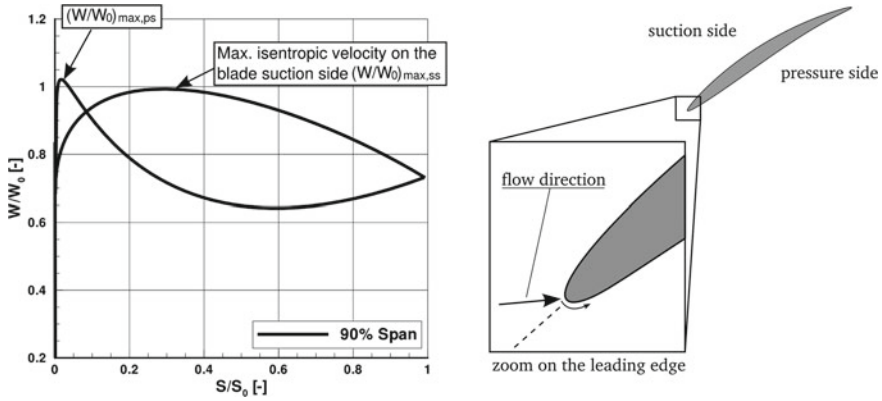


Fig. 11.11 Illustration of negative incidence resulting in a velocity peak on the pressure side

The two objectives are subject to two constraints:

$$Constr_1 = \Delta H \geq \Delta H_{min} \tag{11.11}$$

and

$$Constr_2 = [(W/W_0)_{max,ps} - (W/W_0)_{max,ss}] \leq 0. \tag{11.12}$$

The first constraint (Eq. 11.11) ensures that the designs generated by the optimization program supply the required total head for the design flow rate. The second constraint (Eq. 11.12) prevents that the isentropic velocity objective Obj_2 is not improved at the expense of a higher velocity on the pressure side at the leading edge due to negative incidence, i.e. if the flow impinges on the suction side, which results in a velocity peak on the pressure side (Fig. 11.11).

11.4.5 Results

The results of the optimization are presented in Fig. 11.12, showing both the total head ΔH (Fig. 11.12, left) and the maximum isentropic velocity on the suction side $(W/W_0)_{max,ss}$ (Fig. 11.12, right) with respect to the hydraulic efficiency η_{hyd} . Each symbol in Fig. 11.12 represents one design that has been analyzed by CFD. The square symbols represent the geometries analyzed for the initial database (DOE) prior to the optimization to train the metamodel. The designs generated during the optimization process are the diamond shape symbols. From the initial scattered distribution of the DOE (Fig. 11.12, left), the optimizer generated a large number of designs with high hydraulic efficiency η_{hyd} and minimum required total head (indicated with the horizontal line in Fig. 11.12, left). The selected design of this optimization

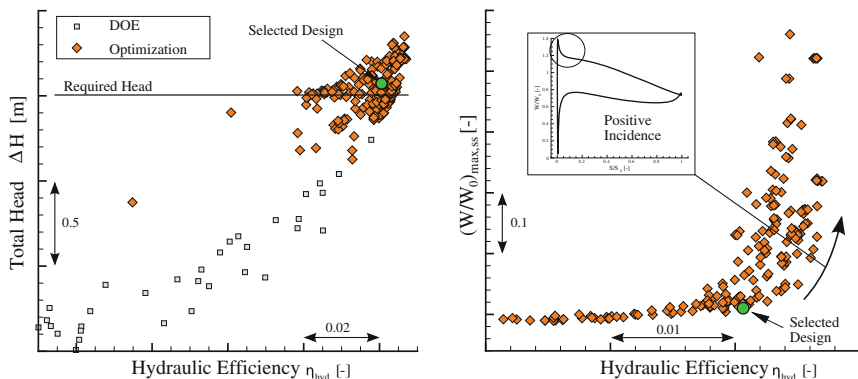


Fig. 11.12 Total Head versus hydraulic efficiency (*left*) 2D objective space: $(W/W_0)_{max,SS}$ versus hydraulic efficiency (*right*)

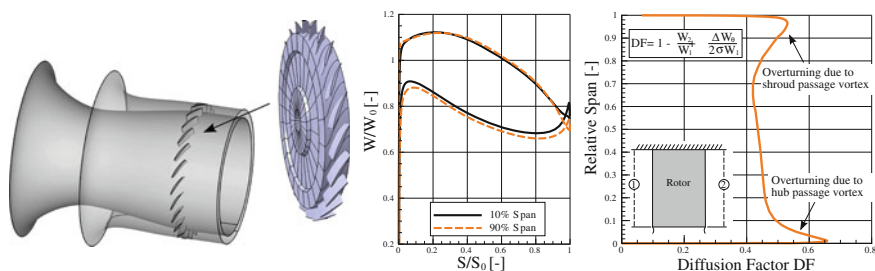


Fig. 11.13 Selected design indicated in Fig. 11.12 with a close up on the rotor (*left*), isentropic velocity distribution at 10 and 90% span (*middle*), span-wise distribution of rotor diffusion factor (*right*)

supplies a total Head, which is above the minimum required value, with high hydraulic efficiency. The reason why this particular design has been chosen is more obvious from Fig. 11.12 right, showing the two-dimensional objective space, i.e. the maximum isentropic velocity on the suction side $(W/W_0)_{max,SS}$ with respect to the hydraulic efficiency η_{hyd} .

In this plot only designs which satisfy the constraints according to Eqs. (11.11) and (11.12) are presented such that the apparent front of designs towards the lower right hand corner is the Pareto front comprising non dominated designs, i.e. no other designs outperform the Pareto optimal designs with respect to both higher efficiency and lower relative velocity. Higher hydraulic efficiency comes at the expense of higher relative velocity due to positive incidence resulting in a velocity peak on the suction side leading edge. In this optimization reducing the isentropic velocity on the suction side, i.e. the relative velocity to limit erosion had a higher priority than improving the efficiency, resulting in the selected design, which is considered as the best trade-off solution of both objectives.

The selected design, which is presented in Fig. 11.13 left, is a high staggered, low aspect ratio rotor ($h/c_{tip} \approx 0.36$) with a solidity in the tip section of $(c/p)_{tip} \approx 1.26$. It is a mid-loaded blade with an equal loading in the hub and tip section and with a smooth diffusion on the suction side as illustrated in Fig. 11.13 middle, showing the isentropic velocity distribution at 10 and 90% span. Additionally, as illustrated already in the 2-dimensional objective space in Fig. 11.12 right, this design has a rather low velocity on the suction side which limits the erosion risk. Figure 11.13 (right) illustrates the mass-flow averaged span-wise distribution of the rotor Diffusion Factor (DF) at design operating conditions. Although the Diffusion Factor introduced by [2]

$$DF = 1 - \frac{W_2}{W_1} + \frac{\Delta W_\theta}{2\sigma W_1} \quad (11.13)$$

using the relative velocities up- and downstream of the rotor and the solidity σ is strictly valid for two-dimensional flows, it is a suitable parameter to estimate off-design tendencies. Except close to the side walls where the flow is overturned due to secondary flows (i.e. due to the hub and shroud passage vortices), the computed rotor Diffusion Factor is below $DF \leq 0.5$, which indicates a sufficient margin towards lower flow rates.

11.4.6 Stator-Diffuser Optimization

Subsequently to the inlet-rotor design optimization, the stator-diffuser has been designed and optimized. A similar parametrization as for the inlet-rotor optimization is used with 18 degrees of freedom, comprising the meridional flow path and blade shape. The design of the rotor is kept constant during this process, but the inlet and rotor are modeled in the CFD during this design effort. The objectives of the optimization are to diffuse as much as possible inside the diffuser with limited losses, while reducing as much as possible the velocity peak on the suction side of the stator vane to limit erosion. The outcome of this optimization is illustrated in Fig. 11.14, showing the meridional velocity with a span-wise distribution upstream of the rotor and the isentropic velocity distribution at 10 and 90% span of the stator vane.

11.4.7 Performance Map

The selected design (Fig. 11.14) has been analyzed further regarding its off-design performance. Although the pump was designed primarily for the design point, it has good off-design characteristics, which is illustrated in Fig. 11.15, showing the Head coefficient

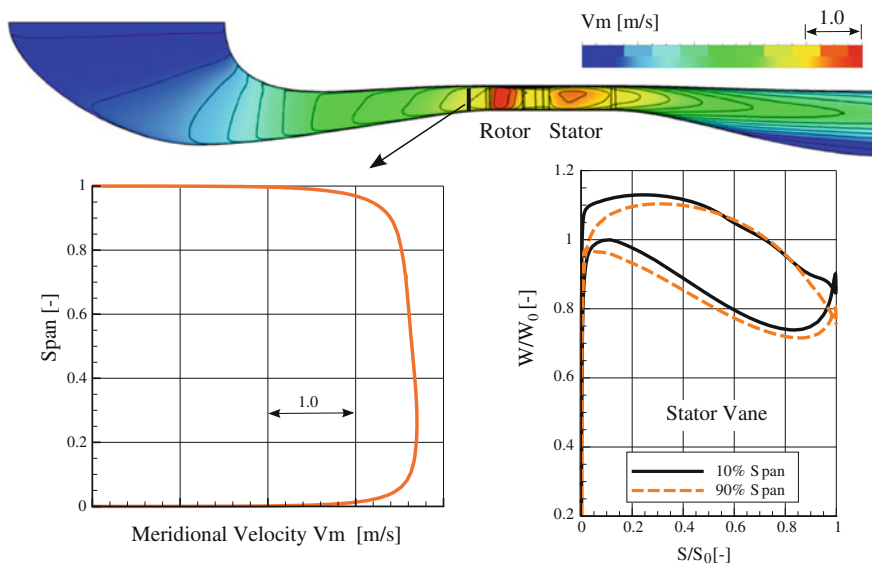


Fig. 11.14 Meridional velocity in the final pump design and isentropic velocity distribution at 10 and 90% span of the stator vane

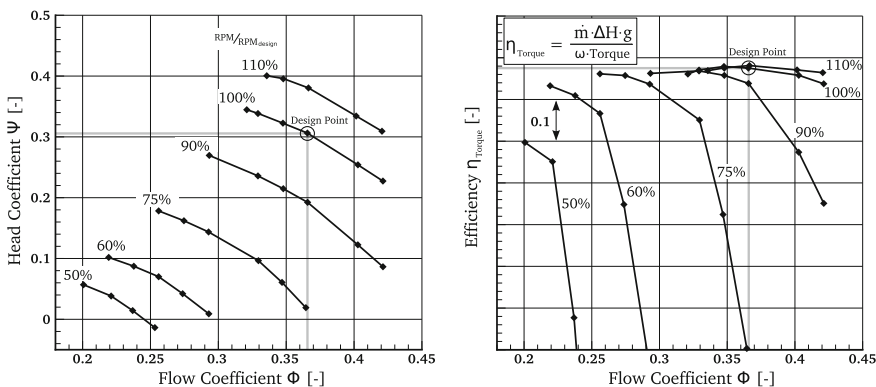


Fig. 11.15 Performance map of the pump

$$\psi = \frac{g \cdot \Delta H}{U_{tip}^2} \tag{11.14}$$

and the efficiency based on the torque

$$\eta_{Torque} = \frac{\dot{m} \Delta H g}{\omega \cdot Torque} \tag{11.15}$$

with respect to the flow coefficient

$$\phi = \frac{V_x}{U_{tip}}. \quad (11.16)$$

The reason for the good off-design behavior is related to the chosen design strategy. The optimization was aiming at limiting the diffusion in the rotor and stator and reducing the incidence of both blade rows resulting in a robust design with an entirely sufficient negative slope ($\equiv \Delta\psi/\Delta\phi$) of the characteristics curve.

11.5 Conclusions

A hydrodynamic optimization based on evolutionary methods is used to design the primary pump of the MYRRHA nuclear reactor. The design approach is aimed at

- maximizing the hydraulic efficiency of the rotor,
- minimizing the pressure losses in the stator and diffuser, and
- reducing the relative velocity in the rotor tip section.

Based on the preliminary 1D optimization, the rotor and stator have been designed in two successive steps keeping the number of design parameters and objectives to feasible values in each optimization run. The outcome is a pump, which supplies the required Head and is respecting the design target of low relative velocity to limit erosion.

The pump has been realized as a moderate specific speed, high hub-to-tip ratio axial pump ($N_s = 70$, $R_{hub}/R_{tip} = 0.88$), although a mixed-flow pump would provide higher hydraulic efficiency according to classical specific speed charts. However, due to the additional complexity of a mixed flow configuration in the manufacturing process, an axial configuration is more attractive.

Although the pump was designed primarily for the design operating point, it has a good off-design behavior, which is the result of the chosen design strategy. The optimization was aiming at limiting the diffusion in the rotor and stator and reducing the incidence of both blade rows resulting in a robust design.

Finally, the use of a two phase approach consisting of a preliminary design phase and a detailed 3D design optimization allows for a strong reduction of the degree of interactions of the design variables, which significantly reduces the design optimization problem at hand. The use of a preliminary search with optimization techniques on a reduced model allows a rapid selection of optimal design variables that are well predicted by the reduced model. The authors advise that a well-thought use of physical models in the early stages of the design process is a prerequisite for a successful detailed design optimization.

References

1. Crouse JE, Sondercock DM (1964) Blade-element performance of 0.7 hub-tip radius ratio axial-flow pump rotor with tip diffusion factor of 0.43. In: NASA TN D-2481, Lewis Research Center, Cleveland Ohio, 1954
2. Lieblein S, Schwenk FC, Broderick RL (1953) Diffusion factor for estimating losses and limiting blade loadings in axial-flow-compressor blade elements. In: NACA RM E53D01, Lewis Flight Propulsion Laboratory, Cleveland Ohio, 1953
3. Miller MJ, Crouse JE (1965) Design and overall performance of an axial-flow pump rotor with a blade-tip diffusion of 0.66. In: NASA TN D-3024, Lewis Research Center, Cleveland Ohio, 1965
4. Montgomery D (2006) Design and analysis of experiments. Wiley, New York
5. NEA: Handbook on lead-bismuth eutectic alloy and lead properties, materials compatibility, thermal-hydraulics and technologies. Nuclear energy agency. <http://www.oecd-nea.org/science/reports/2007/nea6195-handbook.html>. 2008
6. OKBM: Experimental designing bureau of machine building. <http://www.okbm.nnov.ru/> 5 Dec 2013
7. SCKCEN: MYRRHA: Multi-purpose hybrid research reactor for high-tech applications. <http://myrrha.sckcen.be/> 5 Dec 2013
8. Saravanamuttoo H, Rogers GFC, Cohen H, Straznicky PV (2001) Gas turbine theory. Pearson Prentice Hall, Harlow
9. Stepanoff AJ (1957) Centrifugal and axial flow pumps. Wiley, New York
10. Storn R, Price K (1997) Differential evolution - a simple and efficient heuristic for global optimization over continuous spaces. *J Global Optim* 11:341–359
11. Urasek DC (1971) Design and performance of a 0.9 hub-tip-ratio axial-flow pump rotor with a blade-tip diffusion factor of 0.63. In: NASA TM X-2235, Lewis Research Center, Cleveland Ohio 1971
12. Wilcox DC (1993) Turbulence modelling for CFD. DCW Industries Inc, California